



RESEARCH ARTICLE / ARAŞTIRMA MAKALESİ

Seismic Response of Saturated Soils in Gölbaşı District of Adıyaman Province to February 06, 2023 Kahramanmaraş Earthquake

Adıyaman İli Gölbaşı İlçesindeki Suya Doygun Zeminlerin 6 Şubat 2023 Kahramanmaraş Depremine Sismik Tepkisi

Gürkan Özden ^{1*}, Büşra Kartal ²

¹ İstanbul Teknik Üniversitesi İnşaat Fakültesi İnşaat Mühendisliği Bölümü, İstanbul, TÜRKİYE

² Dokuz Eylül Üniversitesi Fen Bilimleri Enstitüsü, İzmir, TÜRKİYE

Corresponding Author / Sorumlu Yazar *: gurkan.ozden@deu.edu.tr

Abstract

On February 6, 2023, two major earthquakes with magnitudes $M_w = 7.8$ and $M_w = 7.6$ occurred along the Eastern Anatolian Fault at nine-hour intervals caused wide-spread damage in 11 provinces Hatay, Kahramanmaraş, Adıyaman, Malatya, Gaziantep, Elazığ, Osmaniye, Şanlıurfa, Diyarbakır, Kilis and Adana. In this study, soil liquefaction, which was extensively observed in Gölbaşı District of Adıyaman Province, is examined specifically in the context of the 6 February Kahramanmaraş ($M_w=7.8$) Earthquake records. As a result of the observations made in the field immediately after the earthquake, eleven microtremor recordings and five boreholes were drilled, and soil samples were recovered. Laboratory tests were carried out on these samples to determine basic soil characteristics. In addition, data from a comprehensive ground survey conducted by İller Bank in 2006 were evaluated. As a result of the analysis of the data, one-dimensional dynamic soil behavior analyses were carried out on the established ground model considered to represent soil profiles with clayey sand layers. The non-linear behavior of the soil and the development of excess pore water pressure were taken into account. In the analyses using Pazarcık TK 4615 Station data, it was determined that the clayey sand layers liquefied, and this finding was compatible with the observations made in the field following the earthquake. Another result of the study was that due to the loss of stiffness and strength due to cyclic shear stresses and induced excess pore water pressure, attenuation instead of amplification occurred in the soil profile, which in turn increased the deformations.

Keywords: Liquefaction, Gölbaşı, Clayey sand, Non-linear soil response, Excess pore water pressure development, 06 Şubat 2023 Kahramanmaraş Earthquake

Öz

6 Şubat 2023'te Doğu Anadolu Fayı boyunca dokuz saat arayla $M_w=7.8$ ve $M_w=7.6$ büyüklüğünde meydana gelen iki büyük deprem Hatay, Kahramanmaraş, Adıyaman, Malatya, Gaziantep, Elazığ, Osmaniye, Şanlıurfa, Diyarbakır, Kilis ve Adana olmak üzere 11 ilde geniş çaplı hasara yol açtı. Bu çalışmada Adıyaman İli Gölbaşı İlçesi'nde yoğun olarak gözlemlenen zemin sıvılaşması 6 Şubat Kahramanmaraş Deprem ($M_w=7.8$) kayıtları özelinde incelenmiştir. Depremin hemen ardından arazide yapılan gözlemler sonucunda 11 mikrotremor kaydı ve 5 sondaj kuyusu açılarak zemin örnekleri alınmıştır. Temel zemin özelliklerini belirlemek amacıyla bu numuneler üzerinde laboratuvar deneyleri yapılmıştır. Ayrıca İller Bankası'nın 2006 yılında gerçekleştirdiği kapsamlı zemin araştırmasının verileri de değerlendirilmiştir. Verilerin analizi sonucunda killi kum tabakalarına sahip zemin profillerini temsil ettiği düşünülen bir zemin modeli kurulmuş ve bunun üzerinde tek boyutlu dinamik zemin davranış analizleri gerçekleştirilmiştir. Zeminin doğrusal olmayan davranışı ve aşırı boşluk suyu basıncının gelişimi analizlerde dikkate alınmıştır. Pazarcık TK 4615 İstasyonu verileri kullanılarak yapılan analizlerde deprem sonrası sahada yapılan gözlemlerle uyumlu olarak killi kum tabakalarının sıvılaşığı belirlenmiştir. Çalışmanın bir diğer sonucu ise tekrarlı kayma gerilmeleri ve aşırı boşluk suyu basıncına bağlı olarak rijitlik ve dayanım kaybı nedeniyle zemin profilinde büyütme yerine azalma meydana gelmesi ve sonuç olarak deformasyonların artmasıdır.

Anahtar Kelimeler: Sıvılaşma, Gölbaşı, Killi kum, Doğrusal olmayan zemin tepkisi, Aşırı boşluk suyu basıncı gelişimi, 06 Şubat 2023 Kahramanmaraş Depremi

1. Introduction

Ground response related structural problems were observed in previous large earthquakes such as 1906 San Francisco ($M_w=7.9$), 1964 Niigata ($M_w=7.6$), 1999 Great Marmara ($M_w=6.6$) and 2020 Samos ($M_w=7.0$) earthquakes. ($M_w=7.6$), 1994 Northridge ($M_w=6.7$), 1999 Great Marmara ($M_w=7.6$) and 2020 Samos ($M_w=7.0$) earthquakes. According to field observations, the damages to structures during strong ground movements is often due to the liquefaction problem of the

bearing soil layers under the foundations. The focus of the selection of Gölbaşı district of Adıyaman province as the study area after the 6 February 2023 Kahramanmaraş earthquake was the intensity of building damage caused by liquefaction. Liquefaction is the failure of the soil when the effective stress approaches zero due to the inability to dampen the pore water pressure, which generally occurs in cohesionless, water-saturated soils under repeated and dynamic loading. Looking at the history of the literature, the observation of liquefaction in cohesionless soils has generally been investigated. However,

liquefaction was observed in the 6 February Kahramanmaraş earthquakes despite the fact that the Gölbaşı soil contains considerable plastic fines.



Figure 1. Satellite view of Gölbaşı.

Some of the studies in the literature on the liquefaction of soils that contain cohesive fine grains are as follows:

Guo et al carried out a study of the liquefaction behavior of silt-clay mixtures with particular emphasis on investigating the inherent liquefaction behavior of sands involving such soils and its dependence on the plasticity index [1]. Their analysis showed that there is a critical value of the plasticity index (I_p) beyond which the cyclic strain rate decreases resulting in higher liquefaction resistance with larger plasticity index. Boulanger & Idriss, suggested that fine grained soils to be handled in two categories from the liquefaction point of view [2]. They called these categories as sand-like and clay-like behavior and explained the transition by means of the correlation between the plasticity index and cyclic resistance ratio (CRR). According to the authors, fine grained soils with $I_p > 8$ are expected to undergo cyclic softening rather than posing liquefaction. Prakash et al., also agreed on the use of I_p as an identifier on liquefaction resistance of fine-grained soils noting that there were gaps on explaining behavior of such soils [3]. The objective of Park & Kim was to investigate the liquefaction resistance of sand samples containing 10% fine grains with different plasticity indices [4]. Cyclic triaxial tests without drainage were performed on loose, medium and dense samples. In order to produce mixtures with different plasticity limits, clean sand with particle sizes ranging from 2 to 0.075 mm was blended with plastic silt and clay. The fines content was kept constant at 10%. The plasticity index of the silt was set to 8, while that of the kaolinite was 18, and the combination of bentonite and silt was 50, with pure bentonite having a plasticity index of 377. Although the plasticity of the fines had a favorable effect on the liquefaction resistance of the loose samples, it reduced the resistance of the dense samples by up to 40% as the plasticity index value increased. This study demonstrates that plastic fines, even when present in small quantities in sandy soils, have a significant effect on liquefaction resistance. The results highlight the importance of considering the plasticity of fines when assessing the potential of soil mixtures for engineering applications and seismic design. Thakur et al., investigated the

dynamic behavior and damage characteristics of low plasticity cohesive soils with an emphasis on the effects of stress history and loading conditions on the behavior [5]. Various two-way strain controlled cyclic triaxial tests were carried out on soil samples collected from Gujarat, India. The research showed the influence of stress history and different loading conditions on the behavior of low plasticity soils at over consolidation ratio (OCR) values ranging from 1 to 4 and cyclic axial strain amplitude ranging from 0.5% to 2%. The results indicated that low plasticity soils were at risk of liquefaction even at low amplitude and high OCR values. While the liquefaction resistance of the soil increased with increasing OCR values, liquefaction resistance decreased with increasing repeated deformation amplitude. Test results showed that cyclic instability occurs prior to flow liquefaction in cohesive soils with low plasticity. During the transition from cyclic instability to flow liquefaction, a two-stage failure response was observed in the soil. The low plasticity cohesive soil initially exhibited 'clay-like' behavior, but later transitioned to 'sand-like' behavior as flow liquefaction commenced. This soil was found to exhibit cyclic instability at excess pore water pressure ratio, r_u , values between 0.85 and 0.95 and flow liquefaction when the r_u value exceeded 0.95.

The aim of this study is to conduct an in-depth analysis of the clay-dominated soil structure of the Gölbaşı region and the effects of earthquake acceleration on soil layers following the Kahramanmaraş earthquakes of February 6, 2023. The study focuses on investigating the liquefaction potential and seismic response of soils containing cohesive fine-grained soils. Soil properties in the region, supported by fieldwork and laboratory analysis are given. The data are used in one-dimensional site response analysis performed to investigate progress of liquefaction along the soil profile and earthquake acceleration on soil layers. Pazarçık Strong Ground Motion Station record is utilized as earthquake excitation.

2. Liquefaction and Lateral Spreading in Gölbaşı

In this study, site visits were made to Gölbaşı district of Adıyaman province as well as Antakya and İskenderun districts of Hatay province following the February earthquakes. As a result of the investigation, it was found that site soils posed liquefaction behavior and as a result of the soil liquefaction, settlements beyond allowable limits and lateral displacements occurred in the area. In this study, however, liquefaction phenomenon that took place in Gölbaşı is taken into consideration.

Building Performance

It was observed in Gölbaşı that numerous buildings have showed large settlements considerable amount of which were of differential type resulting in tilting of the buildings. Although some buildings exhibited punching type settlements that reached to 200 cm, most of them settled on the order of 20 cm with significant rigid rotation component. Liquefaction related failures intensified nearby and along the coastline of the Gölbaşı Lake, which gave its name to the district. It is notable that buildings with basements behaved much better in the region. School buildings two to three storeys high, all with basement floors, did not show rigid rotation. This was also valid for residential type buildings with a single storey basement. It was noted that the ground water table (GWT) which was quite close to the surface prohibited construction of deeper basements. It can also be stated based on field observations that raft foundations avoided structural failures that would emanate from differential settlements. Although some buildings with raft

foundations but with no basements tilted severely and assessed as heavily damaged, none of them collapsed. However, the case was not the same for isolated footings and one-way connected spread foundations. Another interesting feature of widespread liquefaction was the lateral spreading observed at the lake side, which shall be the theme of a separate article. Some of the liquefaction related failures are presented in Figures 2 to 4. Damaged building statistics as obtained from satellite view of the State Land Registry Office web site just after the earthquakes is given in Figure 5. The data presented in the figure, although limited in number, are informative regarding type of damaged buildings. The percentage of recently constructed four and five storey buildings is considerably small indicating positive role of raft foundation during the earthquake. A rather comprehensive spatial damaged building stock distribution as received from the State Disaster and Emergency Management Presidency is shown on Figure 6. As can be seen on the figure almost entire building stock between the lake and the state highway was assessed as moderately or heavily damaged. A final remark regarding building performance on liquefiable soils in this article is that those buildings whose foundations helped to keep the integrity of the structural system survived the earthquake without life loss and total collapse. It appears that the expected interruption of the ground motion by liquefied soil layers like those observed in previous large-scale earthquakes resulted in lower ground accelerations causing much less inertial loads on the structures. Detailed analysis of damage distribution should be subject of a separate article.



Figure 2. Heavily settled building due to liquefaction.

Soil Characteristics of Gölbaşı

The liquefaction prone zone of Gölbaşı consists of predominantly saturated alluvial soil deposits. Soil characteristics were acquired from a comprehensive site investigation study carried out by Geotechnical Investigation Branch Directorate of the Machinery and Drilling Department of the General Directorate of State Provinces Bank to form a basis for future development of Gölbaşı District in 2006 [6], and from a site investigation study conducted following the February 2023 Earthquakes.

As part of the 2006 study, 21 boreholes and 10 geophysical surveys were carried out to determine the soil properties of the Gölbaşı area. The soil properties of Gölbaşı District were determined by examining 174 of the samples taken to the soil mechanics laboratory.

According to the 2006 study, fine-grained soils are identified as high plasticity clay, whereas coarse-grained soils are predominantly silty sand. The USCS classification system shows that high plasticity clay (CH) accounts for 36% of the soils, followed by low plasticity clay (CL) at 24%, clayey sand (SC) at 19%, silty gravel (GM) at 9% and silty sand (SM) at 7%. In addition, 1% of the soils consist of highly plastic clay with organic material, 1% of poorly graded silty clay (GP-GM), 1% well graded silty sand (SW-SM) and 1% being silty and clayey sand (SM; SC). Natural water content of site soils is typically on the order of 25% and the ground water table is close to the surface. It should be noted that natural water content of the clayey soils is slightly higher than plastic limit, which is verified by the site investigation study conducted after the earthquake.

The clayey sand layers were not expected to liquefy according to current liquefaction criteria valid for clayey soils since plasticity indices (I_p) of the clayey sands were above 20, and fine fractions were rarely less than 20%. It was stated that transition from sand-like behavior to clay-like behavior starts at $I_p=2$ and ends at $I_p=8$ beyond which the soil exhibits clay response and not expected to liquefy [2]. The Gölbaşı case, however, does neither fit to this criterion nor the others and will probably stand as a unique case in the liquefaction literature. The mechanisms underlying this phenomenon can only be solved out by means of detailed cyclic laboratory tests. On the other hand, one-dimensional dynamic site response analyses that were performed utilizing excess pore water pressure generation models shed some light on dynamic behavior of site soils as explained in the below given sections of this article.



Figure 3. Soil response indicating bearing capacity loss.

Field Tests

The reconnaissance team planned a site investigation study consisting of five boreholes and consequent soil mechanics laboratory index tests. Locations of the boreholes tagged as DSK1, DSK2, DSK3, DSK4 and DSK5 are shown on Figure 7 along with the pre-earthquake borings. The groundwater level was quite close to the surface being in between 1.0m~1.5m below the grade nearby the shoreline. The SPT data of the DSK boreholes reflect the post-earthquake resistance of the soil profile. A comparison of the pre (i.e. those acquired during Iller Bank 2006 field study) and post earthquake SPT blow counts is made in Figure 8. One may notice that post earthquake SPT

resistances are in general lower than those of Iller Bank data probably since complete dissipation of accumulated excess pore water pressure within the soil layers has not taken place within the time frame of post earthquake field studies. This is especially more evident in the comparison of SPT-N₃₀ values of DSK-2 and SK-9 boreholes that are relatively close to each other nearby the lake.



Figure 4. Lateral spreading on Gölbaşı Lake coastline.

Assessment of Laboratory Tests

Soil samples were transferred to the Soil Mechanics of Dokuz Eylül University Civil Engineering Department. Laboratory tests involved determination water content, grain size distribution, and consistency limits. Variation of water content and consistency limits with depth is presented in Figure 9 on which data belonging to the boreholes shown in Figure 7 are plotted. It is obvious on Figure 9 that natural water content of the samples is often very close to their plastic limit, which is verified by the liquidity index, I_L, variation with depth as may be followed through Figure 10. It can be noticed that clayey soils whether low or highly plastic and sand with clay content pose very firm to medium firm consistency. This finding is contradictory with observed earthquake response of clayey soils. This is later discussed in further sections of this paper.

| No | Storeys | Damaged Buildings |
|----|-------------|-------------------|
| 1 | Five | 3 |
| 2 | Four | 5 |
| 3 | Three | 8 |
| 4 | Two | 18 |
| 5 | One | 4 |
| 6 | Basement | 2 |
| 7 | Soft storey | 3 |
| 8 | Adobe | 3 |
| 9 | Masonry | 12 |

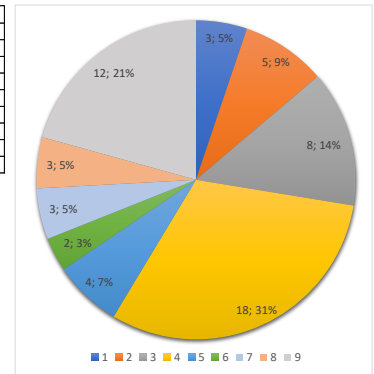


Figure 5. Damage distribution according to building type.

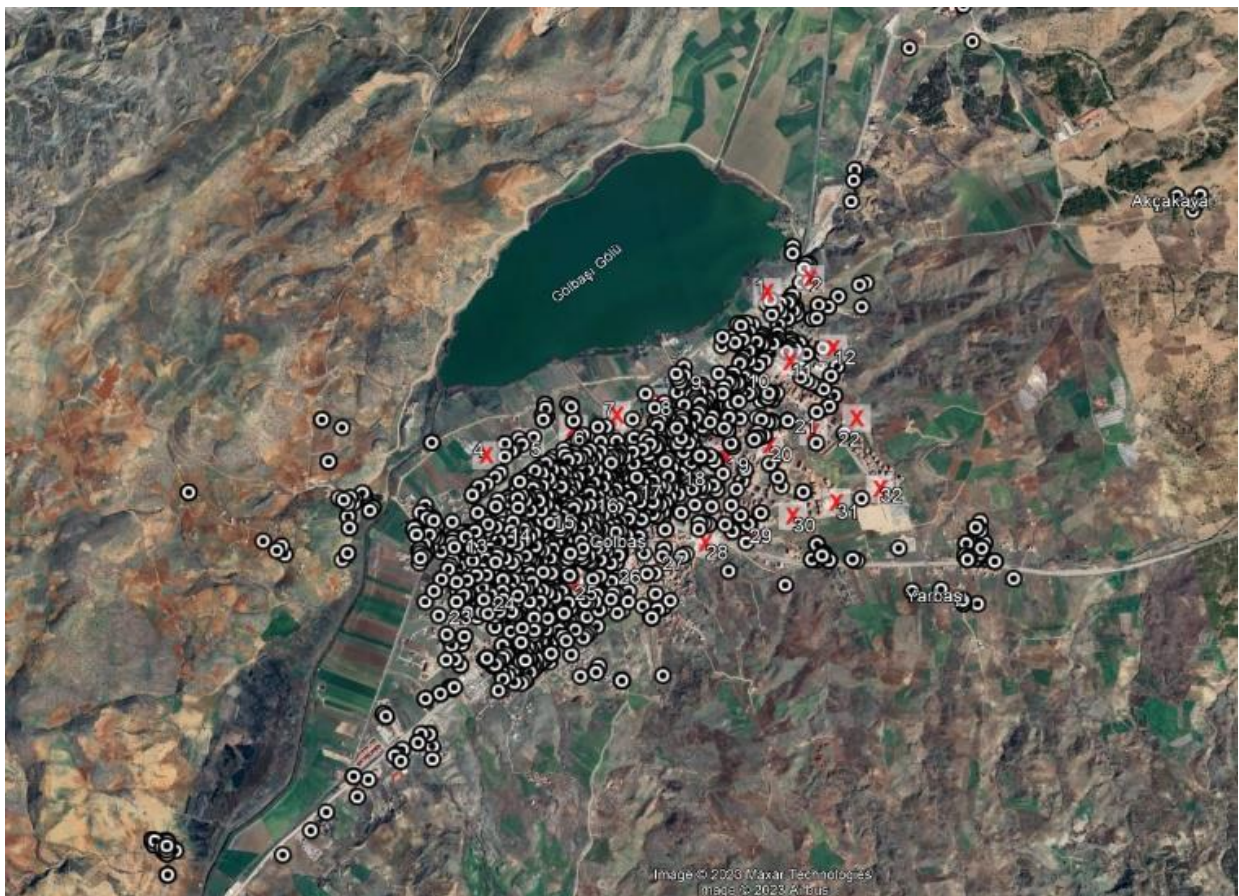


Figure 6. Damaged building distribution in Gölbaşı.



Figure 7. Locations of pre and post-earthquake boreholes (SK-x: pre-earthquake; DSK-x: post-earthquake; -x: microtremor).

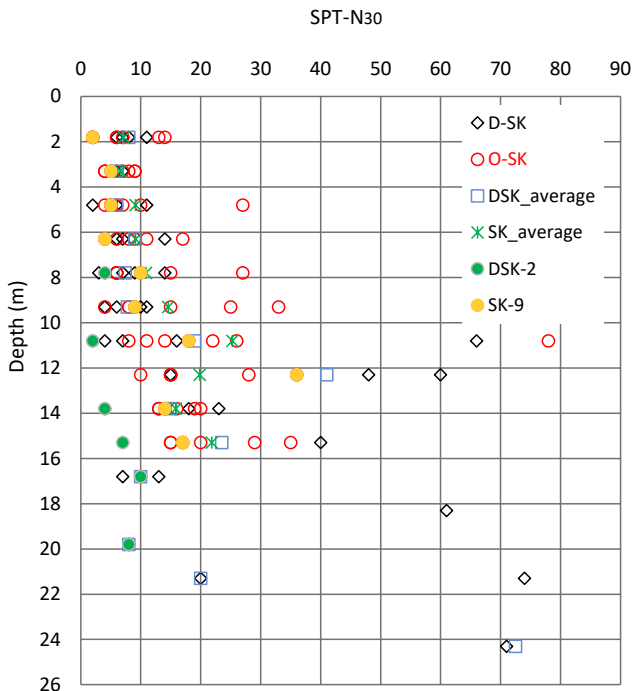


Figure 8. Comparison of pre (SK) and post earthquake (DSK) SPT blowcounts.

A thorough evaluation of the data revealed that acquired samples consisted of fine- and coarse-grained soils almost equally. However, clay soils, either low or highly plastic, rarely homogeneous. Majority of such soils contain gravel and sand fractions at varying percentages. It is noteworthy to mention that 69.6% of clay samples contain more than 20% coarse grains as shown in Figure 11 (i.e. the last data group named as "Fines with Coarse"). There are clayey sands as well whereas silty sands and silty gravels do not dominate the soil profile.

It is quite interesting to see that SPT resistances of both clays and clayey sands do not exactly match with their consistency levels. One expects that medium firm to firm clays pose higher SPT-N₃₀ values in the field [7, 8]. Quite low blow counts were recorded down to 15m depth during post and pre-earthquake site investigation campaigns. Hydrometer tests showed that clay content, C, varies between 20% and 56% lower values corresponding to higher coarse fractions. Limited number of unconsolidated-undrained (UU) triaxial and unconfined compression tests yielded undrained shear strength (s_u) data that vary within the range of 50~105 kPa. Undisturbed soil samples were recovered between 2.10m and 8.70m below the ground surface. Test results are in accordance with firm to medium consistency of clayey soils and with the majority of recorded SPT blowcounts at the sampling depth intervals.

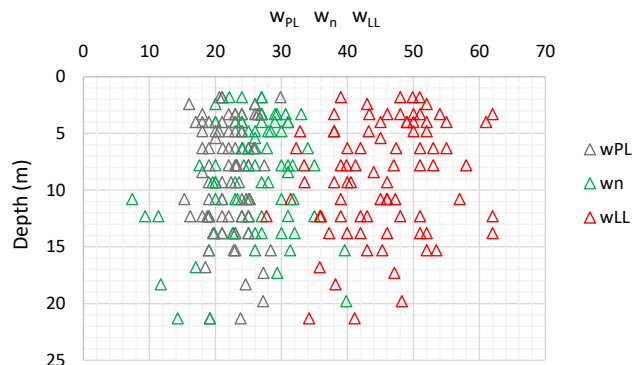


Figure 9. Comparison of natural water content with liquid and plastic limits of the soil samples.

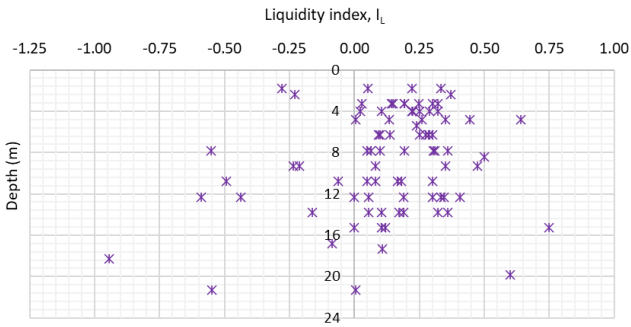


Figure 10. Variation of liquidity index with depth.

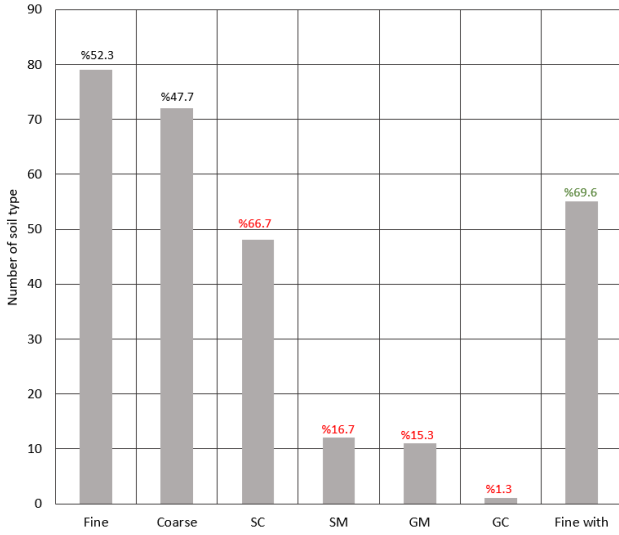


Figure 11. Soil type groups among the test samples.

3. Dynamic Soil Response during Kahramanmaraş Earthquakes

Current state-of-the-art procedure for the determination of liquefaction resistance utilizes field and laboratory data to come up with cyclic resistance ratio (CRR) as a function of fines content, effective stress and earthquake magnitude in addition to standard penetration, cone penetration or shear wave velocity value for a particular soil layer. In this respect, a step-by-step procedure as published by Youd and Idriss [9] is commonly accepted by the geotechnical engineering community. Although it appears that CRR increases with fines content, it has been stated that soil plasticity is not accounted for, and caution is advised while applying correction factors on SPT resistance (Equation 1).

$$(N_1)_{60cs} = \alpha + \beta(N_1)_{60} \tag{1}$$

It should be noted that the “ α ” and “ β ” factors attain constant values as fines content, FC, gets equal to or exceeds 35%. Gölbaşı soils, however, mainly contain more than 30% fines (Figure 12) 66.7% of which exhibit plasticity with I_P varying between 10 and 42. One may note that only samples from one of the post-earthquake boreholes yielded plasticity index values as low as 10. The lowest I_P happened to be 17 in the rest of the evaluated test data. A conventional liquefaction analysis, therefore, may not be indicative regarding the liquefaction potential of Gölbaşı soils that lie between the Malatya Highway and the Lake.

Based on above considerations, one-dimensional dynamic site response analyses were performed using DeepSoil site response analysis software [10] in order to investigate nonlinear behavior

of site soils under Kahramanmaraş strong ground motion excitation records (Pazarçık Strong Ground Motion Station, TK 4615, $V_S=484$ m/s, Soil Class B) considering excess pore water pressure generation. Boreholes and microtremor stations that lie within the encircled area shown in Figure 7 were taken into consideration while establishing the idealized dynamic soil model.

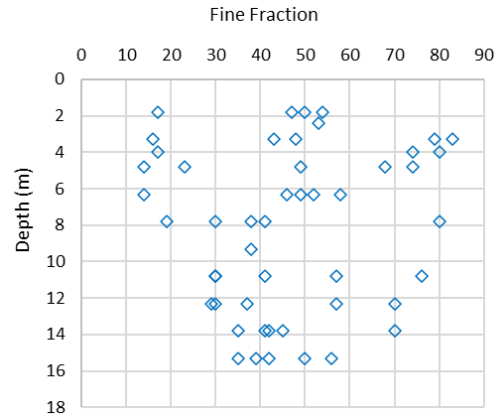


Figure 12. Variation of fines content with depth.

An average plasticity index value of $I_P=20$ was assigned to clayey sand and deep-seated clay layers whereas $I_P=27$ was used for the clay in 5.0m~8.0m depth interval. Angle of internal friction was set to $\phi=26^\circ$ and 24° for the clayey sand and clay layers, respectively. The soil model thus established is given in Figure 13.

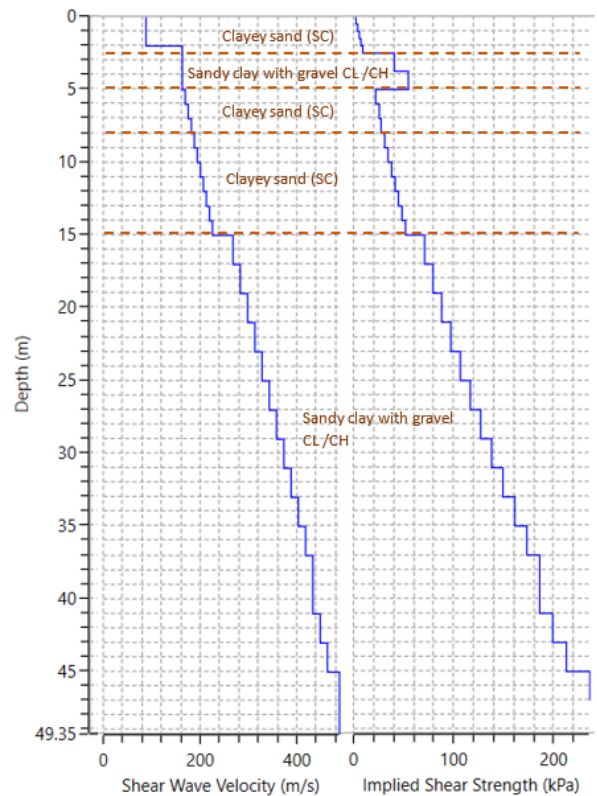


Figure 13. Idealized dynamic soil model.

The soil profile is assumed to be normally consolidated (NC) as can be noted on Figure 13 where both shear wave velocity and shear strength increases with depth. Variation of SPT data with depth are typical to those of the normally consolidated clays.

Filtered and baseline corrected acceleration-time series and 5% damped elastic response spectra of the 06.02.2023 Kahramanmaraş Earthquake ($M_w=7.8$; 04:17 am) are presented in Figure 14. Maximum recorded accelerations along two lateral directions were $a_{max} \approx 0.551g$ and $a_{max} \approx 0.595g$. The records are applied to the elastic engineering bedrock situated at 49m below the ground surface with a shear wave velocity of $V_s=485$ m/s. In this manner the soil conditions at the bottom of the model and the ground motion station matched well. One may note that spectral accelerations exceed the maximum design level elastic spectral acceleration of $1g$ for residential buildings constructed after the year 1998. Older buildings were even

designed for smaller earthquake demands due to the fact that Gölbaşı was classified as the Second Order Earthquake Zone in the 1975 Turkish Earthquake Code forcing the seismic coefficient to be $C=0.08$ for the majority of the buildings. The seismic load reduction factor R_a is on the order of 8.0 for such buildings making the seismic coefficient for total base shear $C \approx 1.2/8=0.15$ on the average for TK4615 acceleration records. Therefore, the total base shear would have been 1.875 times higher than the design level seismic coefficient of $C=0.08$ for pre 1998 buildings had there been no attenuation of the seismic energy during 2023 Kahramanmaraş Earthquake. Fortunately, attenuation took place in liquefied or softened soil zones of Gölbaşı thereby decreasing inertial loads on the buildings. Total collapse was rare for the residential structures that were rated as heavily or moderately damaged on Figure 6 given above.

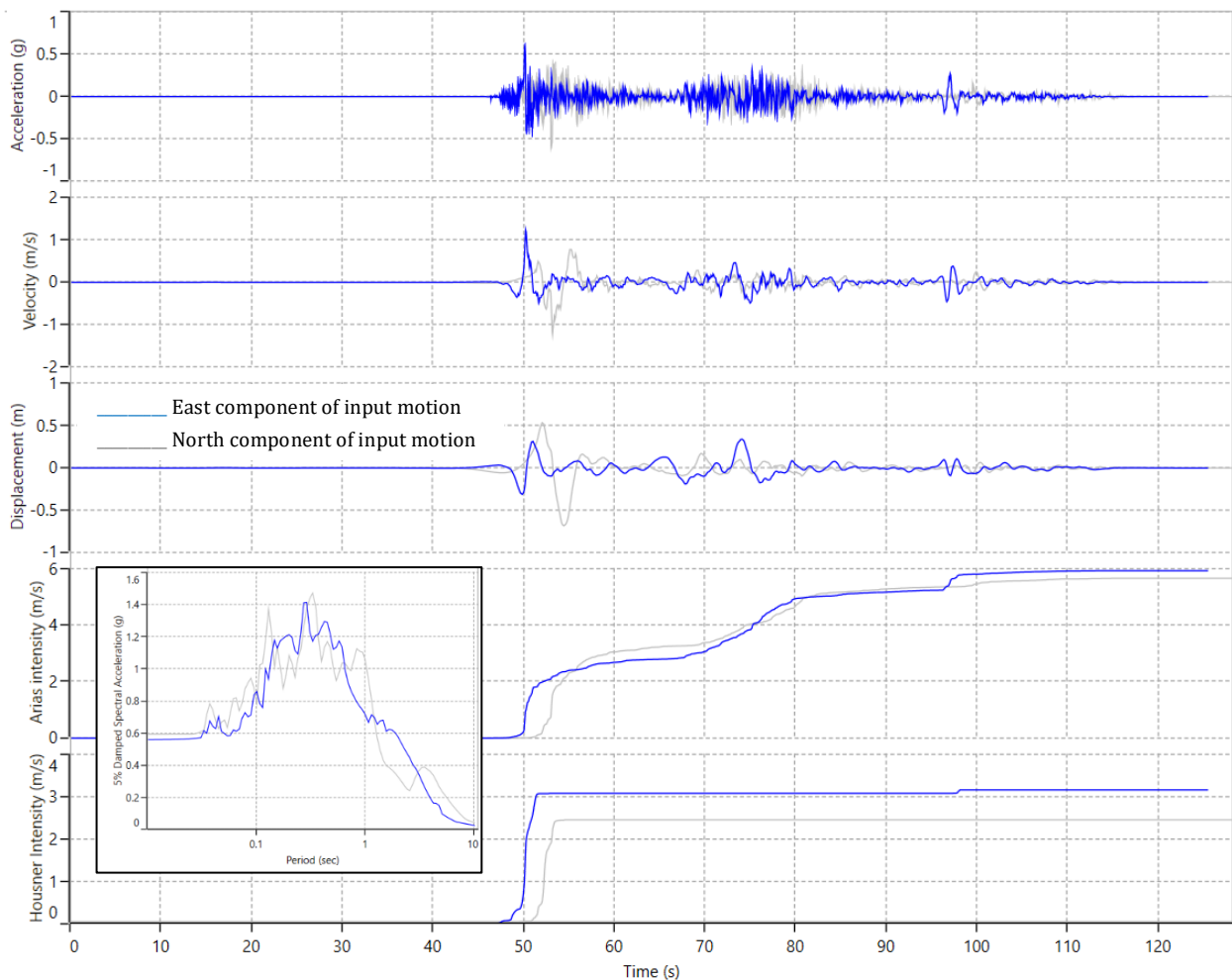


Figure 14. Pazarlık Strong Ground Motion Station (TK 4615) corrected acceleration records and 5% damped accelerations spectra.

The reference backbone and damping curves were constructed obeying to the Darendeli models [11], which are based on resonant column and torsional shear test data compiled at the University of Texas at Austin. In order to provide a more accurate estimate of the shear strength at large strain levels a correction is suggested by Phillips and Hashash [12]. An automatic curve fitting scheme by Groholski et al [13] is embedded in DeepSoil where the shear strength implied by the user is assumed as the limiting value on strain-strength curve. The implied strength and the Darendeli normalized shear modulus backbone and damping curves are then subjected to a

curve fitting procedure (MRDF-Darendeli) to modify the conventional Masing Rules based hysteresis curves in order to avoid overestimation of soil damping at large strains. A more detailed information is available in DeepSoil user’s manual [10] and aforementioned references. Normalized shear modulus backbone and damping curves are provided in Figure 15 for both clayey sand and sandy clay layers at certain depths.

Matasovic and Vucetic approach for clayey soils [15] was preferred as the excess pore water pressure generation and dissipation model to be applied on both clayey sands and sandy clay. Although there is not a widely accepted model for clayey

sands, this attempt was made as a first approximation considering that fine content of clayey soils was no less than 20% exceeding 40% for many sampling depths. Clay content in the fine fraction of three SC samples and a GC sample recovered from different boreholes (i.e. SC samples from SK-9, SK-12 and SK-13; GC sample from SK-5) at 6.3m, 12.3m and 4.0 m, respectively, was determined as 23% for two SC samples, 24% for a SC sample, and 23% for the GC sample.

The residual normalized excess pore water pressure is defined as $(u_N^* = u_N/\sigma'_{v0})$ a function of number of cycles (N), soil's plasticity index (I_p), volumetric cyclic threshold shear strain (γ_{tv}), cyclic shear strain amplitude (γ_c), and empirical coefficients (A, B, C, D, s and r) to account for excess pore water pressure related degradation. General equation is given by Equation (2), and the details of the model may be found in the referred articles.

$$u_N^* = AN^{-3s(\gamma_c - \gamma_{tv})^r} + BN^{-2s(\gamma_c - \gamma_{tv})^r} + CN^{-2s(\gamma_c - \gamma_{tv})^r} + D \quad (2)$$

Volumetric threshold cyclic shear strain $\gamma_{tv}=0.1\%$ was assigned to all soil layers as suggested for normally consolidated clayey soils in the literature [15]. Corresponding empirical coefficients of A, B, C, D, s and r became 7.6451, -14.7174, 6.3800, 0.6922, 0.075 and 0.495, respectively.

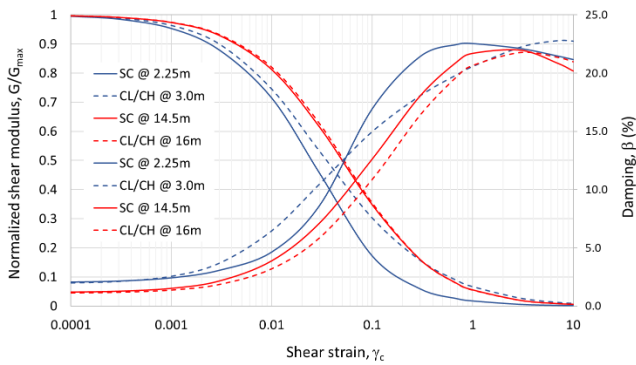


Figure 15. Shear modulus reduction and damping curves.

4. Results and Discussions

One-dimensional site response analyses that were carried out using DeepSoil software yielded some notable results. First of all, the soil profile posed nonlinear response to strong ground motion records of the 06 Kahramanmaraş 2023 Earthquake.

Comparison of the acceleration spectrum at the bottom of the model with that of the ground surface by means of Figure 16 is an indication to nonlinear soil response. It may be noticed on the figure that within the period range of interest (i.e. 0.1s~1.0s) earthquake motion is attenuated whereby amplification took place beyond 1.0 seconds obeying to the fact that elastic fundamental period of the soil profile in the dynamic model is T₀=0.73 seconds, which is continuously enlarged with stiffness and strength degradation as a result of induced shear stresses and excess pore water pressure development.

Variation of peak acceleration and excess pore water pressure ratio ($r_u = \frac{u_e}{\sigma'_{v0}}$) with depth as shown in Figure 17 appears to be dependent on the earthquake direction although peak acceleration and Arias intensity of the north-south and east-west components are close to each other. This response is discussed in the following paragraphs.

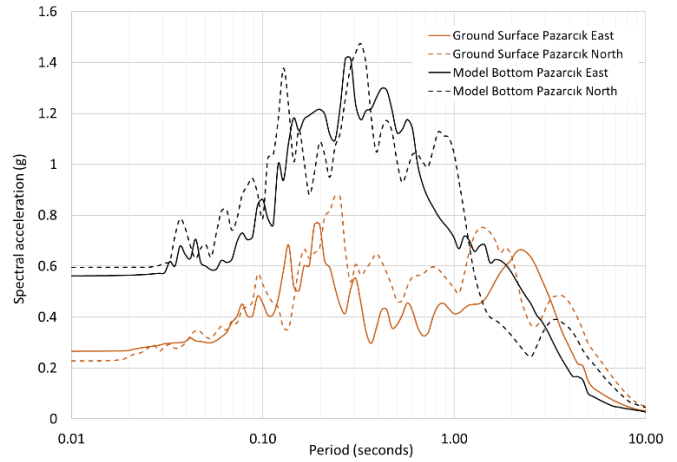


Figure 16. Comparison of spectral accelerations.

Figure 17 shows that considerably higher excess pore water pressures and lower peak accelerations were computed under east-west component of the Pazarçık TK 4615 station within the clayey sand layers between 5.0m-15m below the ground surface. Excess pore water pressure ratio attains values as high as $r_u=0.9$ indicating development of liquefaction. A closer look at the acceleration-time and velocity-time histories to both motion components at the clay layer right below the sandy clay (i.e. @16m) reveal that instantaneous variations in acceleration and velocity is much sharper and larger in the east-west component than that of the north-south component (Figure 18). Doi and Kamai [16] stated that such variations have a more remarkable influence on excess pore water pressure development as compared with cumulative earthquake parameters such as Arias Intensity. One may follow on Figure 18 that sudden increases in excess pore water pressure ratio, r_u , of the east-west component of the earthquake motion well coincides with the sharp increments of velocity-time series of the same component. This aspect of the soil response may be related to the fact that the threshold volumetric strain as defined in the Matasovic-Vucetic model is exceeded at certain values of earthquake velocity pointing out a possible existence of threshold velocity and its relationship with threshold volumetric strain. This subject deserves further study with a companion cyclic testing program on liquefaction resistance of clayey sands with plasticity indices larger than 20.

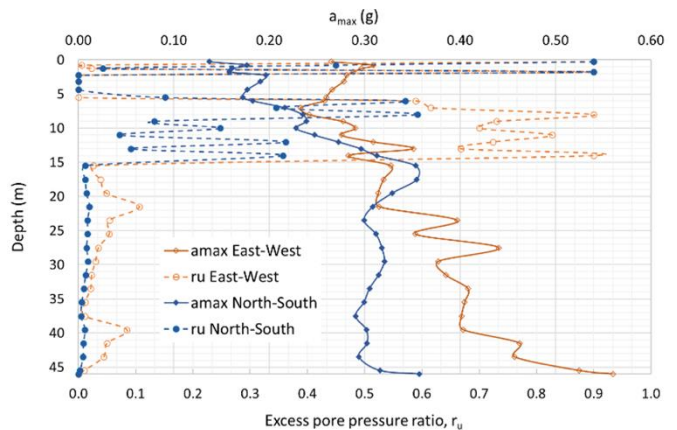


Figure 17. Variation of a_{max} and r_u with depth.

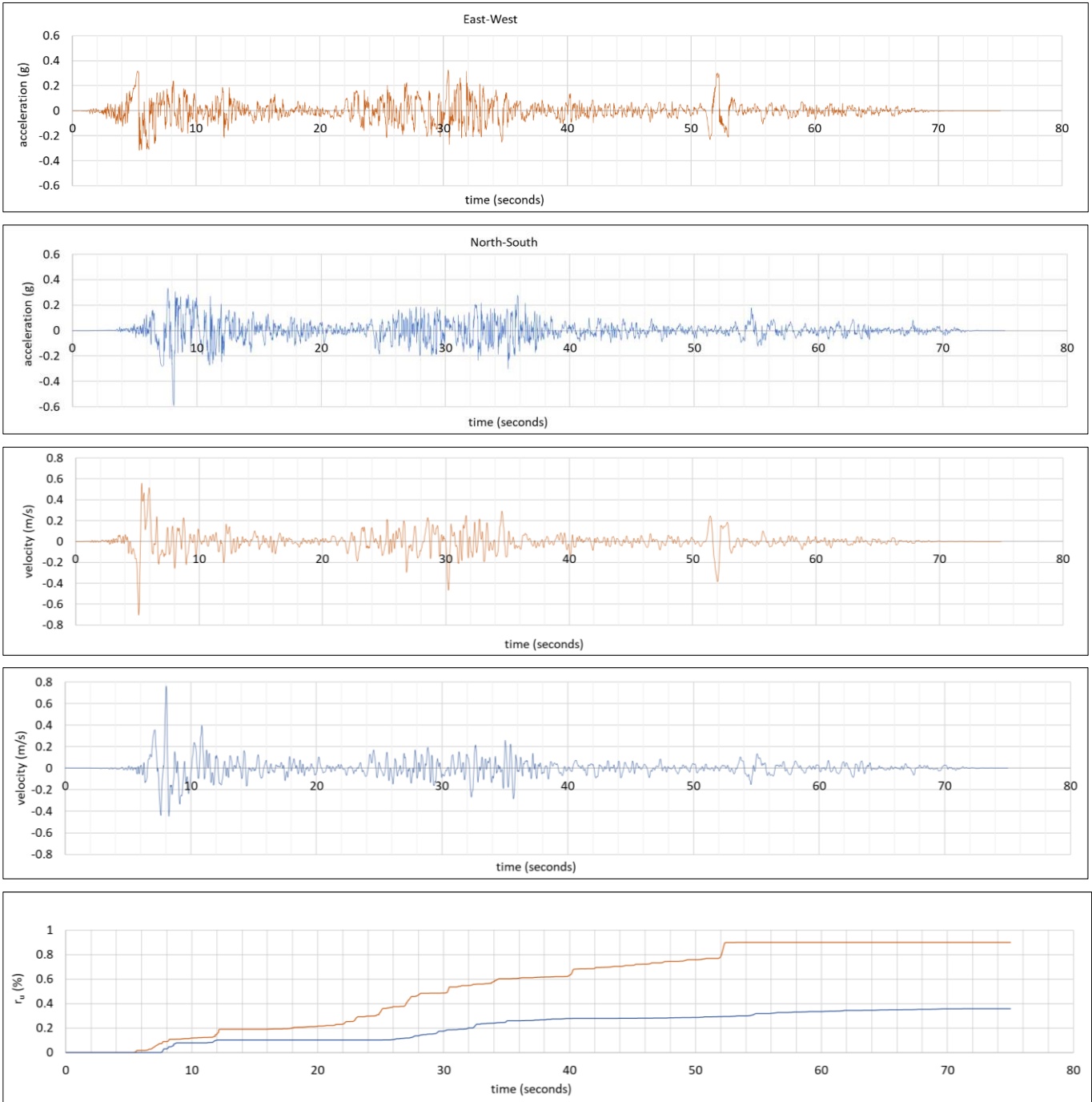


Figure 18. Comparison of acceleration, velocity and excess pore water pressure ratio time series of the Clay Layer #18 @16m acting as an input motion for the 10m thick sandy clay layer above 16m.

5. Conclusions

Gölbası (Adıyaman-Türkiye) exhibited one of the most remarkable examples in the liquefaction case histories during February 6, 2023 Kahramanmaraş Earthquake with a magnitude $M_w=7.8$ that occurred at 04:17 AM. The soil profile where extensive liquefaction took place between the Malatya-Pazarcık Highway and the Lake consists of alluvial and saturated layers of sandy clay, silty sand, clayey sand and silty gravel. The cohesionless soils with silt content would have undoubtedly liquefied during this earthquake like similar soils did in past earthquakes.

The liquefaction of clayey sands, however, makes the the Gölbası Case interesting in this earthquake. Therefore, the authors

focused on the response of clayey sands in this preliminary research study. Matasovic and Vucetic Model for excess pore water pressure generation was applied to both clayey sand and sandy clay layers while performing nonlinear site response analyses. Results show that the model worked equally well for both clayey sands and sandy clays and its excess pore water pressure generation capabilities are highly dependent on the characteristics of the individual strong ground motion.

The East-West component produced higher excess pore water pressure ratio (r_u) inside the 10m thick sandy clay layer located between 5~10 meters below the ground surface as compared with the North-South component of the earthquake. The difference is almost double between the two components. A

closer look at the velocity-time series reveal that pore pressure rise under East-West excitation is correlated with instantaneous variations in the velocity. The North-South excitation, on the other hand, is more modest in this regard. For instance, the increase in the velocity at 52 seconds match well with the rise in r_u taking place in the East-West component.

The fact that SPT blowcounts recorded in the boreholes do not match with the natural water content of the samples reminds that samples would have not been transferred to the soil mechanics laboratory accordingly. The authors, therefore, preferred to model the soil profile to consist of normally consolidated alluvial layers in one-dimensional site response analyses. A detailed research program involving high quality undisturbed samples, geophysical field surveys in addition to other field tests such as SPT and CPT as well as a comprehensive laboratory cyclic testing program will shed more light on the liquefaction mechanism of cohesive soils in Gölbaşı and elsewhere.

Ethics committee approval and conflict of interest statement

This article does not require ethics committee approval. This article has no conflicts of interest with any individual or institution.

References

- [1] Guo, T., & Prakash, S., 2000. Liquefaction of silt-clay mixtures. Proceedings of the 12th World Conference on Earthquake Engineering, Upper Hutt, New Zealand, NZ Soc. for Earthquake Engineering, February, Paper No.0561.
- [2] Boulanger, R. W., & Idriss, I. M., 2006. Liquefaction susceptibility criteria for silts and clays. *ASCE Journal of Geotechnical and Geoenvironmental Engineering*, 132(11), pp.1413-1426. doi:10.1061/(ASCE)1090-0241(2006)132:11(1413).
- [3] Prakash, S., & Puri, V. K., 2010. Recent advances in liquefaction of fine-grained soils. Fifth International Conference on Recent Advances in Geotechnical Earthquake Engineering and Soil Dynamics, May, pp.24-29, San Diego, California, Paper No. 4.17a.
- [4] Park, S. S., & Kim, Y. S., 2013. Liquefaction resistance of sands containing plastic fines with different plasticity. *ASCE Journal of Geotechnical and Geoenvironmental Engineering*, 139(5), pp.825-830. doi:10.1061/(ASCE)GT.1943-5606.0000806.
- [5] Thakur, A. S., Pandya, S., & Sachan, A., 2021. Dynamic behavior and characteristic failure response of low plasticity cohesive soil. *International Journal of Civil Engineering*, 19(2), pp.167-185. doi:10.1007/s40999-020-00560-1.
- [6] Akil, B., Bektaş, İ. B., Şahin, M. S., Saygı, M. S., & Yılmaz, M., 2006. The geology and geotechnical report of sites that are subject to development plans of Gölbaşı Adıyaman Province. Report No: İLB-İ/02-007-002, in Turkish, Bayındırlık ve İskan Bakanlığı, p.255.
- [7] Yaman, G., 2007. Prediction of geotechnical properties of cohesive soils from in-situ tests: An evaluation of a local database. Master of Science Thesis, Middle East Technical University, p.161.
- [8] Bowles, J. E., 1996. *Foundation Analysis and Design*. 5th Edition, McGraw-Hill, ISBN: 0-07-118844-4, 1207 pages.
- [9] Youd, T. L., & Idriss, I. M., 2001. Liquefaction resistance of soils: Summary report from the 1996 NCEER and 1998 NCEER/NSF workshops on evaluation of liquefaction resistance of soils. *ASCE Journal of Geotechnical and Geoenvironmental Engineering*, 127(4), pp.297-313. doi:10.1061/(ASCE)1090-0241(2001)127:10(817).
- [10] Deep Soil, 2022. 1-D Wave Propagation Program for Geotechnical Site Response, Version 7.0.33.0, University of Illinois and Youssef Hashash.
- [11] Darendeli, M. B., 2001. Development of a new family of normalized modulus reduction and material damping curves. PhD Dissertation, The University of Texas at Austin, p.394.
- [12] Phillips, C., & Hashash, Y., 2009. Damping formulation for non-linear 1D site response analyses. *Soil Dynamics and Earthquake Engineering*, 29, pp.1143-1158.
- [13] Groholski, D., Hashash, Y., Kim, B., Musgrove, M., Harmon, J., & Stewart, J., 2016. Simplified model for small-strain nonlinearity and strength in 1D seismic site response analysis. *ASCE Journal of Geotechnical and Geoenvironmental Engineering*, 142(9), pp.1-14. doi:10.1061/(ASCE)GT.1943-5606.0001496.

Acknowledgment

The authors acknowledge the support provided by Housing Development Administration of Turkish Republic Ministry of Environment and Urbanization and Disaster and Emergency Management Presidency of Ministry of Interior and Mehmet Parmaksız (Gölbaşı-Adıyaman) for the post-earthquake site investigation studies. We are also thankful to University of Illinois at Urbana-Champaign Board of Trustees for non-profit distribution of the One-Dimensional Site Response Analysis Software DeepSoil 7.0.

Author Contribution Statement

Author #1 contributed this paper during literature review, conceptualization, model establishment and analysis stages. Author #2, on the other hand, took part in literature review and soil mechanics laboratory tests. We highly appreciate the company and help of Dr. Özgür Bozdağ, Professor Yeliz Yükselen Aksoy, Beril Kılıç, Onur Atlı, Okan Tatar, Nurettin Aytas and İbrahim Kebeli during site visits. Geophysical studies were conducted by Dr. Özkan Cevdet Özdağ of Dokuz Eylül University Earthquake Research and Implementation Center. Authors are indebted to his work during microtremor measurements and analyses of the data.

- [14] Hashash, Y.M.A., Musgrove, M.I., Harmon, J.A., İlhan, O., Xing, G., Numanoglu, O., Groholski, D.R., Phillips, C.A., & Park, D., 2020. DEEPSOIL 7.0, User Manual. Urbana, IL, Board of Trustees of University of Illinois at Urbana-Champaign.
- [15] Matasović, N., & Vucetic, M., 1995. Generalized cyclic-degradation-pore pressure model for clays. *ASCE Journal of Geotechnical and Geoenvironmental Engineering*, 121(1), pp.33-42.
- [16] Doi, I., & Kamai, T., 2020. Relationship between earthquake-induced excess pore water pressure and strong ground motion observed in a monitored fill slope. *Engineering Geology*, p.266. doi:10.1016/j.enggeo.2019.105391.